METHODOLOGY FOR NUMERICAL SIMULATION OF THE LOW CYCLE FATIGUE LIFE

Sushant Bhalchandra PATE, Gintautas DUNDULIS, Paulius GRISKEVICIUS

Faculty of Mechanical Engineering and Design, Kaunas, Lithuania, sushant.pate@ktu.edu,[2] gintautas.dundulis@ktu.lt, paulius.griskevicius@ktu.lt

https://doi.org/10.37904/metal.2024.4878

Abstract

This research presents a development of the methodology for numerical simulation of the low cycle fatigue life. The sensitivity of the number of pairs of the kinematic hardening parameters on the hysteresis loop of the low cycle fatigue behaviour of stainless-steel working under cyclic loading was investigated. An experimental and numerical investigation was carried out on AISI316L steel under 0.18 % strain loading at 20 ° C to predict the fatigue failure of the component. It is observed that the cyclic elastoplastic response of the low cycle fatigue loading improves as the set of kinematic hardening parameters increases. The numerical simulation performed gave the results in good agreement with that of the experimental results. It can be concluded that the presented methodology can be employed for the estimation of the fatigue life of the stainless steel under repetitive strain loading.

Keywords: Low cycle fatigue, finite element method, numerical simulation, kinematic hardening, AISI316L stainless steel

1. INTRODUCTION

Austenitic stainless steel such as AISI316L is used for components operating under fluctuating load at ambient temperature and elevated temperatures, which increases the risk of the low cycle fatigue failure of the components during the operation. Nuclear reactors, pressure vessels, offshore structures, etc., are some examples of such components. Components and structures subjected to stress or strain cycles beyond the elastic limit require an accurate estimation of the fatigue life.

For the research of the low cycle fatigue behaviour of such components, nonlinear kinematic hardening models developed by Armstrong, Frederick and Chaboche are very efficient models for capturing the kinematic hardening behaviour of the components undergoing repetitive/alternative/cyclic loading. It is very important to estimate the parameters of these models accurately to capture the elasto-plastic response of the component during numerical simulation.

Several research studies have been carried out on the estimation of these parameters. Bari et al. [1,2,3], presented the methodology to estimate the kinematic hardening parameters. Moslemi et al. [4], investigated experimentally the low cycle fatigue behaviour and the elastic limit of AISI316L stainless steel pipes exposed to uniaxial and biaxial cyclic loading. They also estimated Chaboche kinematic hardening parameters using particle swarm optimisation and generic algorithm methods. J. Zhou et al. [5], performed the experimental investigation and cyclic constitutive modelling of the low cycle fatigue behaviour of stainless steel at ambient temperature for the strain amplitude range between 0.3 % and 1.5 %. Roslin et al. [6], carried out numerical simulation for low cycle fatigue for strain amplitude ranging from 0.25 % to 0.6% at room temperature on P91 steel by employing finite element method. They estimated the parameters for isotropic and kinematic hardening. The number of components employed to define the kinematic hardening for the material model during numerical simulation plays an important role in capturing the cyclic elastoplastic response of the

material. Therefore, it is necessary to study the influence of the number of kinematic hardening components on the cyclic elastoplastic response.

In this research, a low cycle fatigue experimental and numerical investigation was carried out on AISI316L stainless steel at room temperature for 0.18 % strain. For the numerical simulation kinematic hardening and isotropic hardening is employed. For the research of the low cycle fatigue behaviour nonlinear kinematic hardening models developed by Armstrong - Frederick is used. The sensitivity of the number of pairs of kinematic hardening components in the cyclic stress-strain hysteresis loop is also investigated.

2. MATERIAL AND METHODOLOGY

2.1. Experimental low cycle fatigue test

A single batch AISI316L steel bar with smooth surface and no heat treatment was used to prepare the test specimen. The dimensions of the test specimen are represented in **Figure 1**.

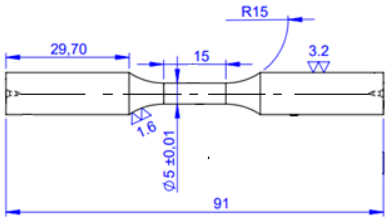

Figure 1 Specimen design for LCF Test

Table 1 Material properties of AISI316L Steel

Temperatuře, °C	Modulus of Elasticity, GPa	Yield Stress, MPa	Poisson's Ratio	Ultimate Tensile Strength, MPa
20	201	231	0.3	554

Table 1 shows the mechanical properties of the material used to prepare the test specimen. Modulus of elasticity and yield stress, which were important for the simulation were estimated using the 1st cycle result from the experiment.The low cycle fatigue experimental test was performed on an INSTRON E10000 test machine with a maximum force of 10kN. The experiments were carried out at room temperature, 20 °C for 0.18 % strain amplitude until failure at approximately 342870 cycles at a frequency of 0.56 Hz.

2.2. Numerical Simulation of Low Cycle Fatigue (LCF)

The numerical simulation of LCF on AISI316L is performed using FEM. The LS-Dyna FE software is used for the FE modelling and simulation of LCF.

2.2.1. Finite Element Modelling.

Considering the axisymmetry of the specimen, during the finite element modelling only the 1/4th portion of the experimental specimen was considered. The FE model of the specimen was prepared by referring to the experimental specimen drawing in **Figure 1**.

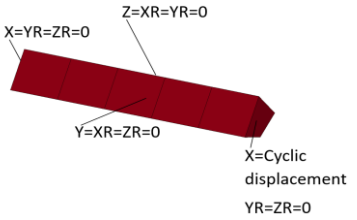

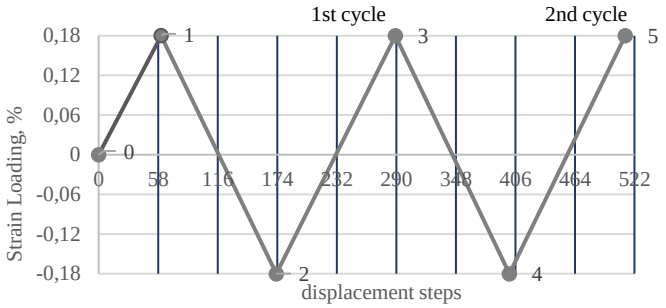

Figure 2 Meshed FE model and boundary conditions **Figure 3.** Displacement for specimen loading

Figure 2 shows the finite element model of the specimen used for the numerical investigation along with the applied boundary conditions. Five elements of 8-nodes constant stress solid element were used for this modelling.

2.2.2. Specimen loading

Figure 3 represents the relative displacement applied to the specimen during the numerical simulation. The displacement was applied to the front face in the X-axial direction of the specimen as shown in **Figure 2**.

The full reversed triangular wave form displacement as represented in **Figure 3** was applied to the specimen according to the recorded strain controlled LCF test data. One full cycle consists of 232 steps which consists of 116 steps for tension part and 116 steps for compression part of the cycle. The first loading cycle begins from the rest position of the sample (i.e., 0 % strain) and proceeds as points '0-1' which is quarter cycle, therefore it consists of 58 steps and '1-2-3' is one full cycle which totally consists of 232 steps followed by the second cycle '3-4-5' and it repeats.

2.2.3. Material Modelling

For capturing the required elastoplastic response as per the experimental results, isotropic hardening along with the kinematic hardening was applied for the material model. In LS-Dyna software there is a predefined material model (Damage3) that employs combinations of isotropic and kinematic hardening.

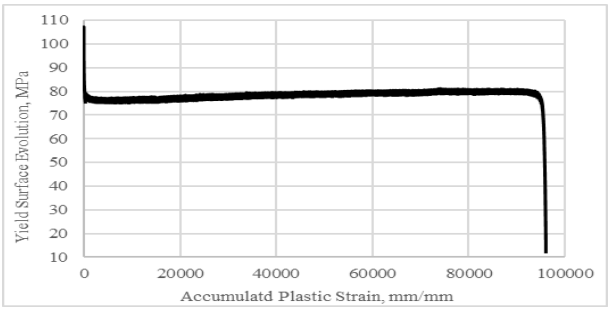

Figure 4. Isotropic Hardening Curve Used in the LS-Dyna

Figure 4 shows the isotropic hardening curve employed for the numerical simulation. The X axis and the Y-axis represent accumulated plastic strain, $\bar{\varepsilon}_p$ and evolution of yield surface, σ respectively.

$$\sigma = \sigma_{max,i} - \sigma_{y0} \quad (1)$$

Where: $\sigma_{max,i}$ is maximum stress for the current cycle, σ_{y0} is Initial Yield stress and

$$\dot{\bar{\varepsilon}}^{pl} = 2N\Delta\varepsilon_{pl} \quad (2)$$

where N represents number of cycles and $\Delta\varepsilon_{pl}$ plastic strain range (%). Equations 1 and 2 represent the evolution of the yield surface and the accumulated plastic deformation, respectively, used for the calculation of the isotropic hardening curve shown in **Figure 4**. The Damage3 material model in LS-Dyna uses the Armstrong-Frederick kinematic hardening model equation 3.

$$\dot{\alpha}_j = \frac{2}{3} C_j \dot{\varepsilon}^{pl} - \gamma_j \alpha_j \dot{\bar{\varepsilon}}^{pl} \quad (3)$$

where C is kinematic hardening (MPa), γ represents exponent for kinematic hardening, $\dot{\varepsilon}^{pl}$ is plastic strain, $\dot{\bar{\varepsilon}}^{pl}$ accumulated plastic strain and α_j is black stress. The kinematic hardening components were estimated using the tension loading part of the stabilised cycle, which was 171000. The kinematic hardening components are estimated according to equation 4.

$$\dot{\alpha} = \sum_{j=1}^{n} \left[\frac{2}{3} C_j \dot{\varepsilon}^{pl} - \gamma_j \alpha_j \dot{\bar{\varepsilon}}^{pl} \right] \quad (4)$$

where n = 1,2,3. For n = 1, 2 and 3, one, two, and three back stress were considered.

Table 2 Kinematic Hardening Parameters Used in Ls-Dyna

Set (n)	C1 (MPa)	Y1	C22 (MPa)	Y2	C30 (MPa)	Y3
1	503150	1198	-	-	-	-
2	450000	950	269000	1860	-	-
3	150500	1680	450650	2530	10560	1360

Three sets of Armstrong-Frederick kinematic hardening components were estimated and presented in the **Table 2**. The aim of this research was to investigate the sensitivity of the stress-strain hysteresis loop on the number of components employed to describe the kinematic hardening of the material. The kinematic hardening components are employed in pairs of two parameters, i.e., one kinematic hardening modulus and one kinematic hardening exponent. Therefore, it can be observed in **Table 2**, set 1 consists of one pair of components, set 2 and set 3 consists of two pairs and three pairs respectively.

3. RESULTS

To present the experimental results a curve was plotted maximum stress versus number of cycles for maximum stress, minimum stress, mean stress and stress amplitude of each cycle. **Figure 5** shows the plotted curve for experimental results of the low cycle fatigue test on AISI316L stainless steel for a strain amplitude at room temperature. After several initial cycles, the material shows softening behaviour; this can be observed as the maximum stress per cycle reduced after several initial cycles. The specimen failed after 342 870 cycles due to the fracture in the centre of the gauge length. The results obtained were used to estimate the material parameters to define the numerical simulation material model.

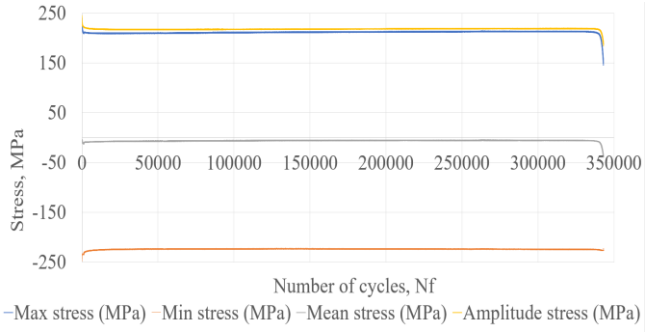

Figure 5 Experimental results., stress versus number of cycles curve

The material parameters such as yield stress, modulus of elasticity, kinematic hardening parameters (KH), and isotropic hardening curve were estimated using the experimental data. The simulation was carried out by applying one set, two sets, and three sets of KH components that can be observed in **Figures 6–8**.

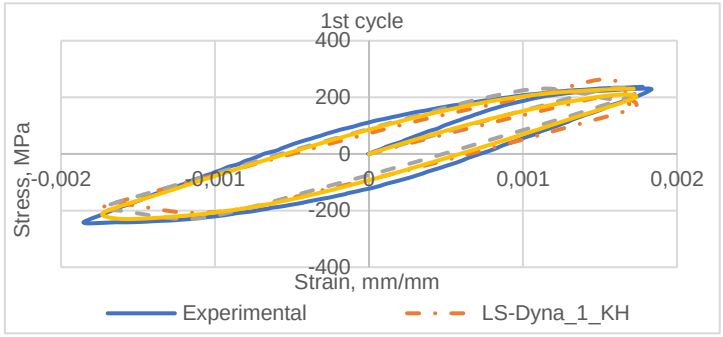

Figure 6 Comparison of stress versus strain hysteresis for the first cycle of the 0.18 % strain model

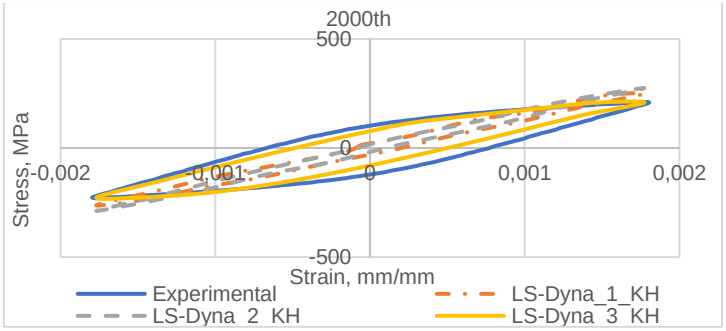

Figure 7 Comparison of stress versus strain hysteresis for the 2000th cycle of the 0.18 % strain model

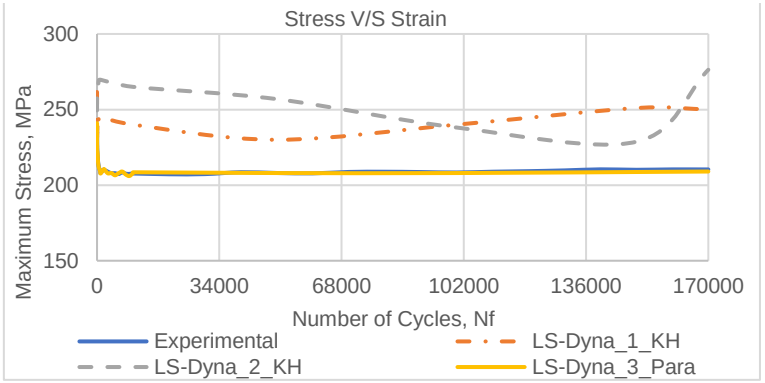

Figure 8 Comparison between experimental and simulation stress versus number of cycle results

Figures 6 and **7** presents the stress versus strain hysteresis loop for the first and 2000th loading cycles successively. **Figure 8** presents the maximum curve stress versus the number of cycles for the experimental and simulation results. It was observed for the stress-strain loop that the curve estimated by applying three components to determine the kinematic hardening parameters gave very close simulation results to the experimentally estimated results. For sets 1 and 2 of the kinematic hardening components, not many changes were observed in the shape of the curve, but changes in the stress levels were observed. For the set 3 significant changes in the shape stress strain levels were observed. Similar observations were recorded for the maximum stress of the cycle versus the number of cycles curve plotted in **Figure 8**.

4. CONCLUSION

Experimental and numerical simulation of low cycle fatigue in AISI316L stainless steel at room temperature for a constant strain amplitude of ±0.18 %. The recorded experimental results showed a reduction in the maximum stress of each cycle after the initial phase of increase in maximum stress until the 60th cycle, which represents the phenomenon of cyclic softening of the material and the material was proved to fail by the occurrence of the fracture in the centre of the gauge length of the experimental specimen at the loading cycle 342870. The numerical model for the simulation is prepared employing the finite element method. The data for the modelling of the system were estimated using the recorded experimental data. The yield stress, modulus of elasticity, isotropic hardening curve, kinematic hardening parameters etc. were estimated as the experimental data and results.

Three sets of parameters were estimated as set 1, 2, and 3 consisting of one pair, two pairs, and three pairs of the kinematic hardening components, respectively. Numerical simulations were performed for each set of kinematic hardening components separately. The simulation results were validated by comparing them with the experimental results. It was observed that the stress-strain cyclic loop and the maximum stress versus number of cycles curve both got better shaped, and the value of the stresses estimates the value close to the experimental values as the number of pairs of kinematic hardening components increases, i.e. the curve for three sets of KH parameters is very close to the experimentally estimated curve. The numerical simulation results had deflection by 3.8 % for the maximum stress level.

Referring to the numerical simulation results, it can be concluded that the presented finite element methodology for the numerical simulation of the low cycle fatigue of steel under constant amplitude repetitive cyclic loading to estimate the approximate fatigue life of the components operating under similar conditions.

ACKNOWLEDGEMENT

Authors are gratefully the INCEFA-Scale consortium for providing the data and the expert panel for the assessment of the individual data sets. The experimental testing and numerical simulation research were funded by the Euratom research and training program 2019-2020 under grant agreement No 945300.

REFERENCES

[1] BARI, S., HASSAN, T. Anatomy of coupled constitutive models for ratcheting simulation. Int. J. Plast. 2000, vol. 16, pp. 381–409.

[2] BARI, S., HASSAN, T. Kinematic hardening rules in uncoupled modeling for multiaxial ratcheting simulation. Int. J. Plast. 2001, vol. 17, pp. 885–905.

[3] BARI, S., HASSAN, T. An advancement in cyclic plasticity modeling for multiaxial ratcheting simulation. Int. J. Plast. 2002, vol. 18, pp. 873–894.

[4] MOSLEMI, N., GOL ZARDIAN, M., AYOB, A., REDZUAN, N., RHEE, S. Evaluation of Sensitivity and Calibration of the Chaboche Kinematic Hardening Model Parameters for Numerical Ratcheting Simulation. Applied Sciences. 2019, vol. 9, no. 12, 2578. https://doi.org/10.3390/app9122578.

[5] ZHOU J., SUN Z., KANOUTÉ P., RESTRAINT D., Experimental analysis and constitutive modelling of cyclic behaviour of 316L steels including hardening/softening and strain range memory effect in LCF regime. International Journal of Plasticity. 2018, vol. 107, pp. 54-78, ISSN 0749-6419. https://doi.org/10.1016/j.ijplas.2018.03.013.

[6] Roslin, M.A.A., Ab Razak, N., Alang, N.A. Numerical Simulation of P91 Steel Under Low-Cycle-Fatigue Loading. J. Fail. Anal. and Preven. 2023, vol. 23, pp. 520–528. https://doi.org/10.1007/s11668-022-01574-8.